JOURNAL OF MATERIALS SCIENCE 16 (1981) 3461–3469

γ' particle coarsening and yield in Alloy 800

M. VITTORI
Laboratorio Caratterizzazione Materiali CNEN, CSN Casaccia, CP 2400, Rome, Italy

The age strengthening of Alloy 800 by ordered particles of γ'-$Ni_3(Al, Ti)$ phase has been studied by using both transmission electron microscopy and room-temperature tensile tests on aged specimens. The samples have been aged in the temperature range 525 to 650° C up to a maximum time of 10^4 h. Two groups of samples with different Ti/Al ratios have been investigated in order to obtain more reliable information on the role played by these alloying elements on the age-hardening behaviour. The γ' linear dimension increases with time, t, as $t^{1/3}$ and an activation energy of 70.0 kcal mol^{-1} was derived from the temperature dependence of the coarsening rate. The particle volume-fraction, as measured by electron microscopy, has been found to remain constant on ageing in the temperature range 525 to 600° C. The increase in the critical shear stress due to the γ' particles is found to agree quantitatively with the equations of Brown and Ham which describe hardening by ordered particles. Antiphase boundary energies of 227 and 279 mJ m^{-2} have been measured, respectively, for the two groups of samples investigated.

1. Introduction

The effect of alloying elements present in small quantities (less than 1%), namely Ti, Al and C, on the ageing behaviour of Alloy 800 has received a particular attention, since liquid-metal fast-breeder reactor (LMFBR) steam generator tubes experiencing a service temperature around 525° C can be manufactured using this alloy [1–4]. The main effect of carbon is the precipitation of $M_{23}C_6$ carbides on the grain boundaries, but is not taken into account in this work. The purpose of the present paper is to present preliminary experimental results on the role played by Ti and Al on the Alloy 800 strengthening by γ'-phase $Ni_3(Al, Ti)$ particles. In fact, this kind of homogeneous precipitation has been observed after ageing in the temperature range of about 500 to 700° C [2–4].

The γ'-particles have the ordered LI_2 crystal structure and are structurally coherent with the fcc matrix lattice; Ni atoms occupy the faces of the fcc lattice while Ti and Al are statistically distributed at the lattice corners.

In γ/γ' alloys, dislocations have been observed to travel in pairs; the first creates an antiphase boundary (APB) by cutting those particles which cross their slip plane, the second restores the order since it travels through the same particles on the same slip plane [5–8].

Brown and Ham [9] reviewed several papers and derived expressions for the expected increase in the critical shear stress, $\Delta\tau_c$:

$$\Delta\tau_c = 0, \qquad r_s < \pi Sf/4\gamma; \quad (1)$$

$$\Delta\tau_c = (\gamma/2\mathbf{b})\{(4\gamma r_s f/\pi S)^{\frac{1}{2}} - f\}, \qquad \pi Sf/4\gamma < r_s < S/\gamma; \quad (2)$$

$$\Delta\tau_c = (\gamma/2\mathbf{b})\{(4f/\pi)^{\frac{1}{2}} - f\}, \qquad r_s > S/\gamma; \quad (3)$$

where γ is the APB energy, f is the precipitate volume-fraction, S is the line tension of the dislocations, $\mathbf{b}$ is the Burgers vector of the dislocations and r_s is the average particle planar radius ($r_s = (2/3)^{1/2}r$ where r is the average particle radius). These expressions are valid for spherical precipitates which are randomly distributed in space, are stress free, are coherent with the matrix, and are elastically isotropic and have a volume-fraction such that $f \ll 1$.

On the other hand, Orowan loops are often observed in peak ageing conditions [5–7], so that $\Delta\tau_c$ is expected to decrease with increasing r for very large particles.

To use the above expressions requires a knowl-

0022–2461/81/123461–09$02.90/0

TABLE I Chemical composition of the two groups of samples (all values are given in wt %)

Batch number	C	Al	Ti	Ni	Cr	Mn	Si	Cu	S	P	N	Fe
761	0.03	0.30	0.58	33.3	21.9	0.62	0.56	0.10	0.016	0.009	0.013	Balance
760	0.03	0.23	0.58	34.4	22.1	0.56	0.60	0.10	0.005	0.009	0.009	Balance

edge of how the average particle size changes with time and temperature. The classical Lyfshitz and Slyozov [10] and Wagner [11] (LSW) theory of diffusion-controlled particle coarsening, has been widely used in the past to describe coherent particles growth. According to this theory, in supersaturated solid solutions very fine particles nucleate and, after some time, the precipitating elements reach their equilibrium concentration in the matrix. Later on, the particles coarsen with large precipitates growing at the expense of small ones and at practically constant volume-fraction. This process is driven by the decrease of the total interface free energy. For this stage the average particle radius r is predicted to vary with time according to

$$(r - r_0) = Kt^{\frac{1}{3}}, \quad (4)$$

where r_0 is the average radius at the onset of the coarsening, t is the ageing time and K is the coarsening rate constant. The LSW theory is strictly applicable only when the volume-fraction of precipitate tends to zero. To overcome this limit, Davies *et al.* [12] recently improved the above theory by taking into account in the formulation of the coarsening rate constant, the effect of the coalescence events between particles which touch each other during the growth. In this formulation, the Lifshitz and Slyozov encounters modified theory (LSEM), it is found that both the coarsening rate constant and the particle-size distribution are affected by the precipitate volume-fraction, while Equation 4 for the time dependence of the average radius is still valid.

Brailsford and Wynblatt [13] have recently published the results of a theoretical study devoted to diffusion-controlled particle growth, where, excluding from consideration the effect of encounters, the same growing law as that of the LSW theory is obtained but, as in the LSEM theory, both the coarsening rate constant and the particle-size distribution are predicted to depend on the particle volume-fraction. However, in their theory, the dependence on the particle volume-fraction of the above parameters, arises directly from the formulation of the kinetic equation; despite formulation of the coarsening rate constant results similar to the LSEM theory, the value of the constants α and β appearing in the expression for K are different in the two theories. The coarsening rate constant K is expressed by:

$$K = (6\gamma_s C_e V_m^2 D\beta/RT\alpha)^{\frac{1}{3}}, \quad (5)$$

where γ_s is the matrix–particle interface free energy, C_e is the equilibrium concentration of the precipitating elements (in equilibrium with a flat surface), V_m is the precipitate molar volume, D is an effective diffusion coefficient which is a function of the diffusion coefficients of the precipitating elements in the matrix [11], R is the gas constant and T is the temperature; α and β are constants depending on the particle volume-fraction; with $\beta = 1$ and $\alpha = 27/4$, Equation 5 becomes the classical LSW coarsening rate constant.

The approach to the study of precipitation hardening of Alloy 800 used in the present work is based on a systematic examination of aged samples, both of their mechanical properties and microstructure. Two groups of samples of differing Ti/Al ratio have been studied in order to obtain more significant results.

2. Materials and experimental procedure

The chemical compositions of the two groups of samples are reported in Table I. Both samples were solution treated at 1010° C for 30 min, air cooled, and then aged at 525, 550, 575, 600 and 650° C (with the temperature controlled to within ± 3° C). Specimens machined from the aged material were subjected to tensile tests at room temperature in a Wolpert tensile machine at a strain rate of 3×10^{-3} min^{-1}. The 0.2% proof stress, $\sigma_{0.2}$, was derived from the recorded stress–strain curves. The tensile tests were performed on samples solution-treated and aged for 100 h, 500 h, 1000 h, 2000 h, 5000 h and 10 000 h.

Slabs of thickness 1 mm, cut from the screw ends of the tensile specimens were mechanically thinned to 0.08 mm. Discs of diameter 3 mm, punched from the thinned slabs, were submitted to double-jet electropolishing in a 10% percloric acid solution in ethylene glycol with an applied voltage of 18 V. The resulting specimens, suitable

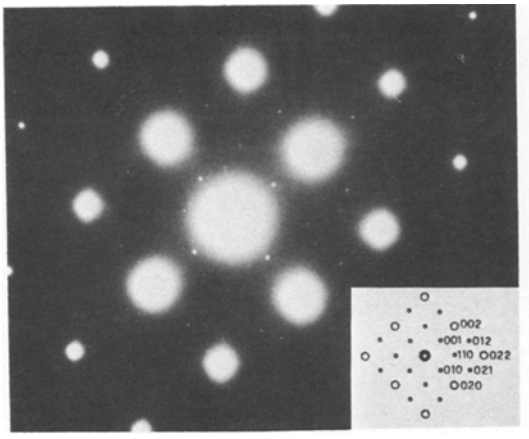

Figure 1 Electron diffraction pattern of aged Alloy 800 showing {1 0 0} and {1 1 0} superlattice reflections, Batch 761 aged for 2000 h at 600° C.

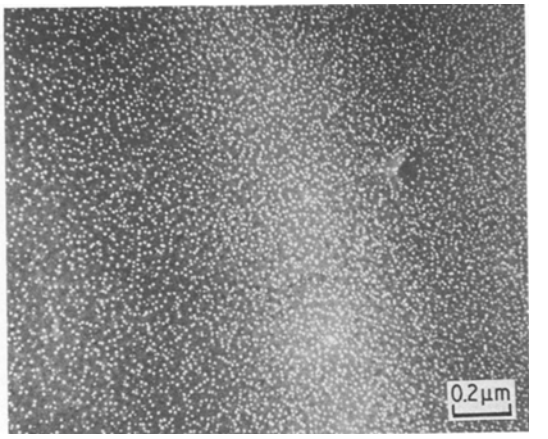

Figure 3 Dark-field image of γ'-phase, Batch 761 aged for 10 000 h at 550° C.

for transmission electron microscopy, were examined with a Siemens Elmiskop 102 electron microscope equipped with a double tilt–lift specimen stage and operated at 100 kV.

By using a superlattice reflection, dark-field images of the γ'-phase precipitates were obtained. An electron diffraction pattern containing γ' superlattice spots is shown in Fig. 1. Typical images of both large ($r = 6.9$ nm) and small ($r = 2.8$ nm) particles are shown in Figs 2 and 3, respectively. This technique proved to give sharp images of γ' particles having an average radius as small as 1.5 to 2 nm.

By analysing the photographic plates with a Metal Research QTM 720, the particle-size distribution was obtained in the following way; the threshold of the QTM 720 machine was defined in order to select only the dark areas on the plate corresponding to the γ' particle images. This operation is not affected by a large error owing to the sharp contrast shown by the particle images. After that, the QTM 720 machine was switched to the count mode and the total number of particles in the area being analysed was obtained. The histogram of the particle diameters was obtained by changing step-by-step the threshold of the sizing device; in this way only those particles with diameters larger than the imposed one were counted. The number of particles in a particular column of the histogram, the nth column, was obtained by subtracting the total number of particles counted with the threshold at the nth position from the total number counted with the threshold at the $(n-1)$th position. Since the linear dimension selected by the sizer device is measured in units of picture points, a calibration of the instrument is required to obtain absolute values. This operation was performed with the aid of a standard plate with circular black spots of accurately measured size. The average radii were computed from the histograms; each computation covered a population of more than 4000 particles. The γ' phase volume-fractions were measured in the overaged specimens; the corresponding size distributions were corrected for the overlapping and truncation effects according to Hilliard [14]. The correction resulted in a negligible shift in the average radius but gave an increase in the volume-fraction of about 10 to 20% depending on the thickness of the observed specimen, which in turn was measured from the projected length of dislocations in pile-up or from slip traces. An

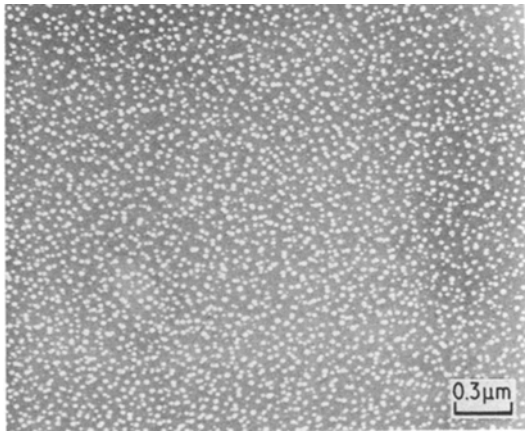

Figure 2 Dark-field image of γ'-phase, Batch 761 aged for 2000 h at 650° C.

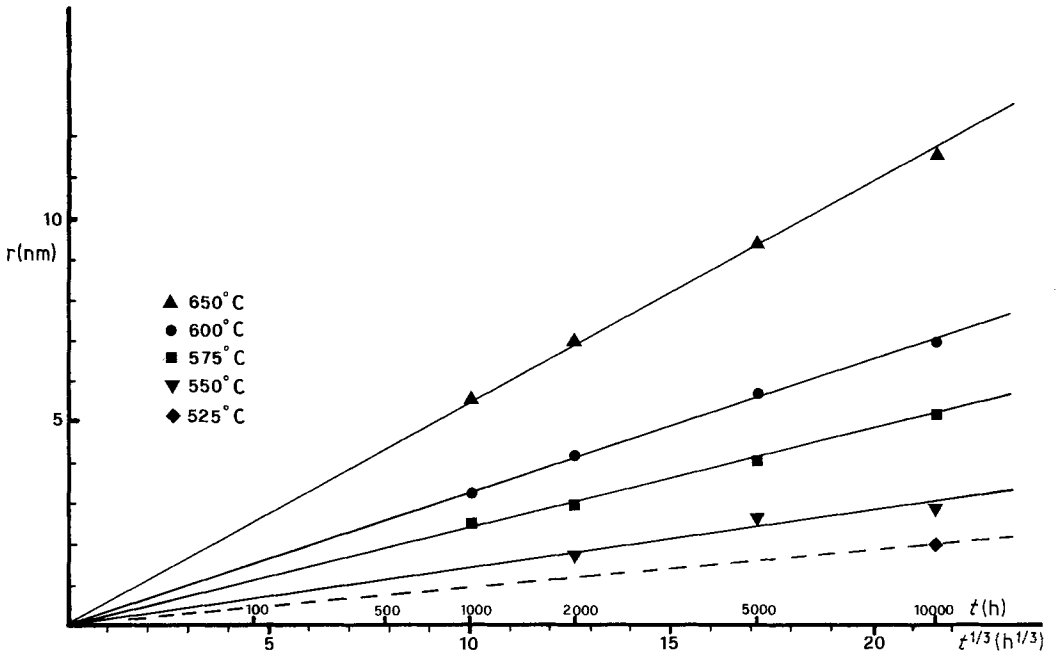

Figure 4 Growth of the γ' particles during ageing of Batch 761. The experimentally determined average radius is plotted against $t^{1/3}$ for all the ageing temperatures investigated.

approximate error around 10% can be assumed for the experimental volume-fraction determinations.

3. Experimental results

3.1. Coarsening behaviour

The γ' particles appear to be spherical in all the observed specimens. The experimental average radii, r, for the samples in Batch 761 (Ti = 0.58 wt %, Al = 0.30 wt %) are reported in Fig. 4. A growing law of the type $t^{1/3}$ fits the data. The extrapolated r_0 is so small that it can be neglected in describing the particle growth. The volume-fractions, f, are listed in Table II for all the ageing temperatures investigated. It can be noticed that in specimens aged between 525 and 600° C the precipitate volume-fraction remains constant, within experimental error; at 650° C it is found to decrease.

TABLE II Data concerning the coarsening of the γ'-phase particles

Batch number	T (° C)	K (nm h$^{-1/3}$)	F (vol %)
761	650	0.55	1.8
761	600	0.33	2.7
761	575	0.24	2.8
761	550	0.14	2.9
761	525	0.09	2.8
760	600	0.29	2.4
760	575	0.20*	
760	550	0.13*	
760	525	0.08*	

*Extrapolated value.

The coarsening rate changes with temperature as predicted by Equation 5 in which the temperature-dependent terms are C_e, D and, obviously, T itself. The diffusion coefficient D is given by $D = D_0 \exp(-Q/RT)$ where D_0 is a frequency factor and Q is an activation energy depending substantially on the activation energies for diffusion of Ti and Al in the matrix [11].

In the analysis herein reported, C_e is assumed constant from 525 to 600° C, owing to the constancy of the γ' volume-fraction. This assumption causes a slight error if the chemical composition of the γ' phase is not constant over the ageing temperature range. With the above assumption Q can be computed inserting the above expression for D in Equation 5. The following expression is obtained:

$$\ln(K^3T) = \text{const} - (Q/RT). \qquad (6)$$

The $\ln(K^3T)$ experimental values plotted against T^{-1} fit a linear relationship, from which a value of 70.0 kcal mol^{-1} is obtained for Q (see Fig. 5).

For the samples in Batch 760 (Ti = 0.58, Al = 0.23), both the γ'-particle coarsening rate and the volume fraction have been experimentally

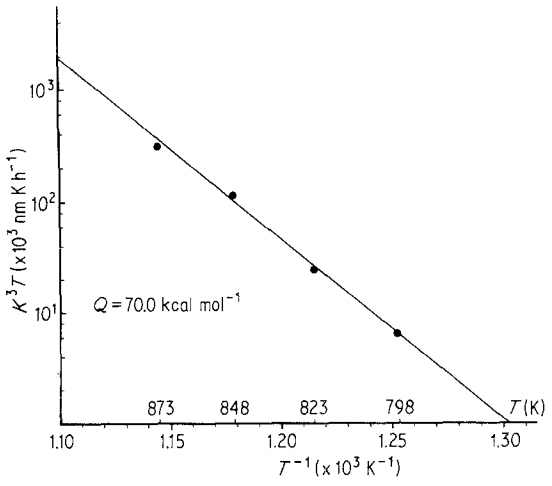

Figure 5 Determination of the activation energy for coarsening. The K^3T values concerning Batch 761 are plotted against T^{-1}.

measured in specimens aged at 600° C. Assuming the same particle growing behaviour in both batches, the γ' coarsening rates in the temperature range covered by the above assumptions have been computed from Equation 6 using the experimental value for Q. The volume fraction has been considered to be the same as that measured at 600° C. The corresponding set of data is reported in Table II.

3.2. Precipitation hardening

The increase in the critical shear stress caused by the γ' particles has been assumed to be $\frac{1}{2}\Delta\sigma_{0.2}$. This parameter is estimated by

$$\Delta\sigma_{0.2} = \sigma_{0.2a} - \sigma_{0.2st}, \quad (7)$$

where $\sigma_{0.2}$ is the 0.2% proof stress and the subscripts a and st refer to aged and solution-treated material, respectively. Owing to the small volume fraction of the γ'-phase the contribution of the solid solution strengthening is considered to be constant.

According to Equation 1 the plotting of $\Delta\tau_c$ against $r^{1/2}$ should be linear for small $r^{1/2}$. The slope and the intercept are, respectively, given by

$$\Delta\tau_c/r^{\frac{1}{2}} = 0.51\gamma^{\frac{3}{2}}f^{\frac{1}{2}}S^{-\frac{1}{2}}b^{-1}; \quad (8)$$

$$\Delta\tau_c(r^{\frac{1}{2}} = 0) = -\gamma f/2b. \quad (9)$$

The APB energy depends on the chemical composition of the hardening particles [9]; as the γ' volume fraction is constant for the specimens aged between 525 and 600° C and assuming also in this case that the γ' chemical composition remains constant with temperature, $\Delta\tau_c$ is expected to depend only on $r^{1/2}$.

In Figs 6 and 7, $\Delta\sigma_{0.2}$ is plotted against $r^{1/2}$ for the two batches, respectively; the experimental points refer to specimens aged in the range 525 to 600° C. It can be seen that the experimental data fit a linear relationship well and that the intercept is clearly negative.

Assuming that edge dislocations control the plastic flow [7, 9] and that the Poisson ratio, ν, is 1/3, then the line tension S is $S = (G\mathbf{b}^2/8\pi)\ln(R/\mathbf{b})$, where G is the shear modulus and R is the outer cut-off radius of dislocations for which the Friedel mean free dislocation length is used [6, 9]. S depends to a small extent on r through the outer cut-off radius R, so that over the particle size range considered here, the value $S = G\mathbf{b}^2/(2.1\pi)$, obtained under average conditions (average f, average r) has been used for all the calculations. By measuring the elastic modulus and by assuming $\nu = 1/3$, a G value of 7.3×10^4 MPa has been obtained. A Burgers vector, $\mathbf{b}$, of 0.25 nm is taken. Finally the values of the slope and of the intercept have been obtained for both batches by a least-square fit analysis of the experimental data. γ can be computed from Equations 8 and 9. Since scattering of data is expected to produce a larger variation in the intercept than in the slope, the APB energies computed from the latter appear more reliable. However it can be seen that the values of γ are not very different from those obtained from the former. The numerical results from both are reported in Table III. The upper deviation from linearity should occur at $r = (3/2)^{1/2}S/\gamma$; for larger r, $\Delta\tau_c$ is expected to be constant, according to Equation 3. The computed values of the above parameters reported in both Table III and in Figs 6 and 7, show a satisfactory agreement with the experimental data for both batches. In Figs 6 and 7 the expected Orowan stresses, as given by [9], are also reported:

$$\Delta\tau_c = (0.4/\pi)(G\mathbf{b}/L)\{\ln(X/b)\}/(1-\nu), \quad (10)$$

where X is an outer cut-off radius and L is the average effective particle spacing in the slip plane. In the calculation, L is replaced by f and r and it is assumed that $\nu = 1/3$ and $X = 2r_s$ [9]. The Orowan stress is expected to be reduced by a factor of a half for paired dislocations [8, 15]. Both functions are plotted in Figs 6 and 7.

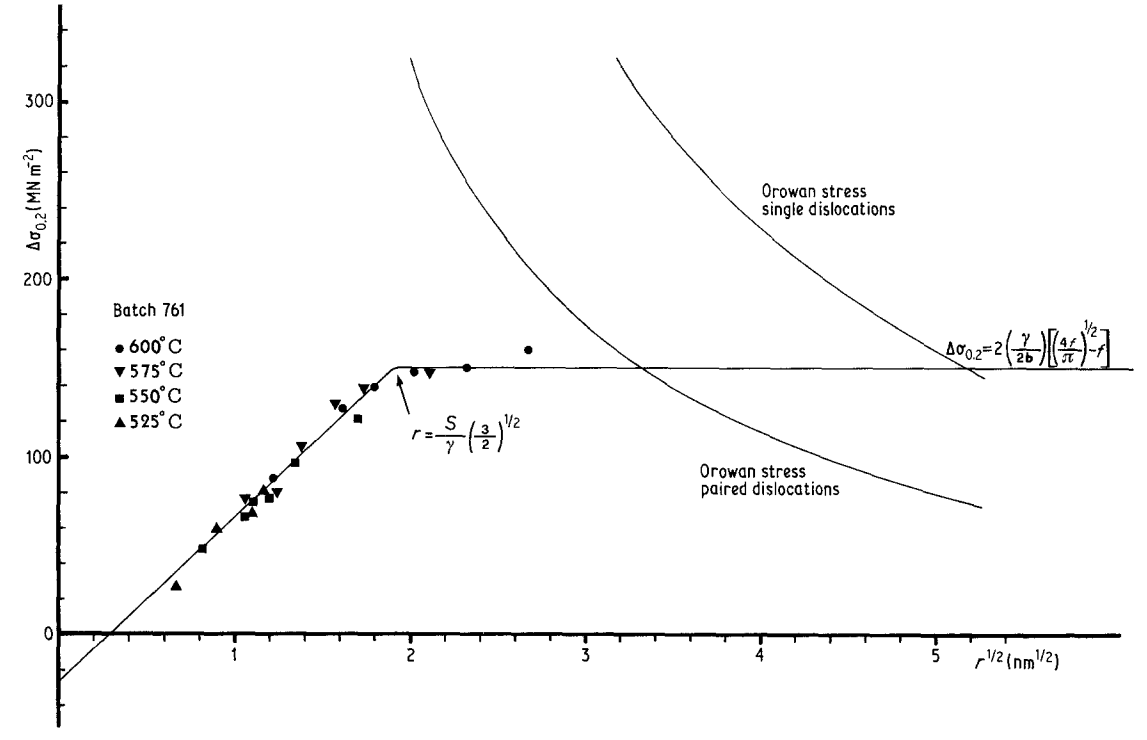

Figure 6 The relationship between particle size and increase in the 0.2% proof stress for Batch 760. The constant value for $r > (3/2)^{1/2}S/\gamma$ is computed using the γ-value obtained from the slope of the linear interpolation of the curve in the small r region.

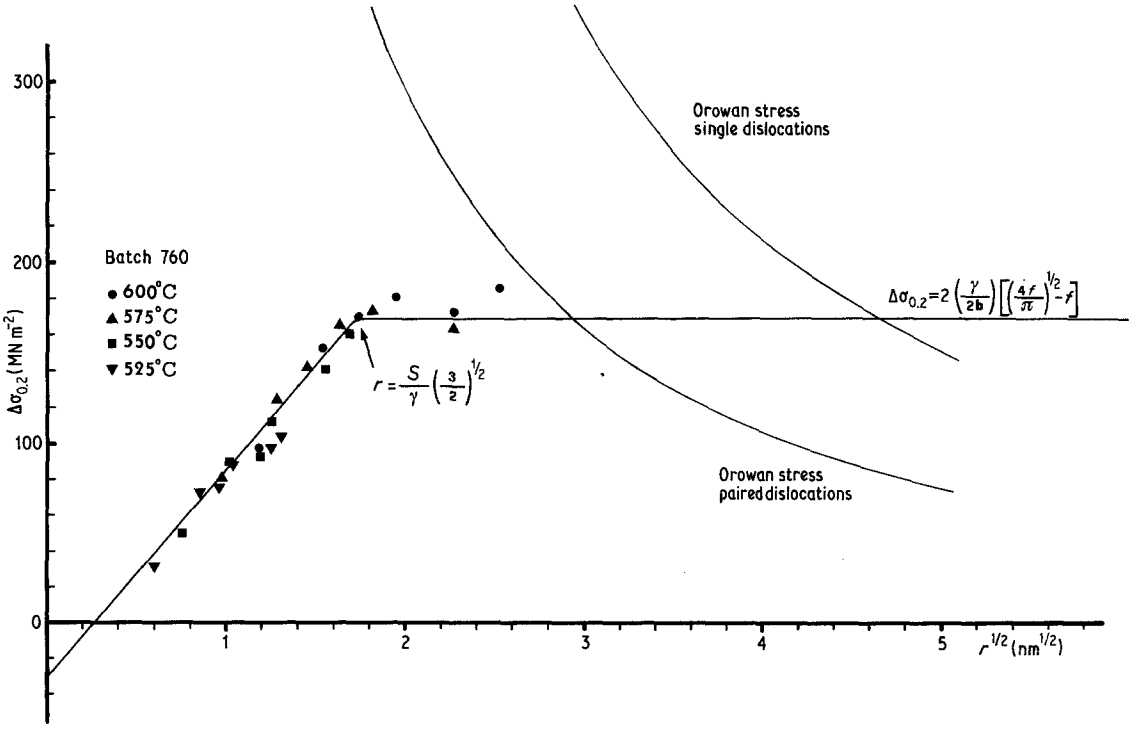

Figure 7 The relationship between particle size and increase in the 0.2 proof stress for Batch 761. The constant value for $r > (3/2)^{1/2}S/\gamma$ is computed using the γ-value obtained from the slope of the linear interpolation of the curve in the small r region.

TABLE III Data concerning the hardening behaviour. The γ-values are obtained from the experimental data while the values in the two last columns are computed from Equations 1 to 3

Batch number	γ(mJ/m^2)		$\Delta\tau(r_S > S/\gamma)$ (MN/m^2)	$r = (3/2)^{1/2}S/\gamma$(nm)
	Slope	Intercept		
761	227	196	73	3.7
760	279	260	84	3.0

4. Discussion

4.1. Coarsening behaviour

The average particle size of γ' in Alloy 800 gives results with time that increase as $t^{1/3}$; this power-law dependence is predicted by all the particle growing theories outlined in the introduction (LSW, LSEM, Brailsford and Winblatt). However, only from our data it is impossible to decide which theory of these theories gives the best fit to the experimentally determined coarsening data. In fact, to compute the rate constant, K, the equilibrium concentration, C_e, and the effective diffusion coefficient, together with the matrix particle interface free energy, should be known. The coarsening rates found in Alloy 800 are low compared with other γ/γ' alloys [16, 17], owing to the low C_e value in this alloy. The coarsening rates seem to be affected by the Ti and Al contents, since there is a difference of about 10% between K values for the two batches at the same ageing temperature.

The temperature dependence of the coarsening rate is well described by Equation 3 in which Q has a value of 70.0 kcal mol^{-1}. The initial hypothesis concerning the constancy of the γ' chemical composition, used in the computation of Q, seem now more reliable in the light of the independent results concerning the APB energy, which also appear to remain constant over the same temperature range. On the other hand, it is noticed that the Q-value of the alloy is quite close to those measured from the coarsening behaviour of γ'-phase both in binary alloys (for example, NiAl: 65.4 kcal mol^{-1} [18]; NiTi: 67.5 kcal mol^{-1} [19]) and in more complex alloys (for example, Udimet 700: 64.5 kcal mol^{-1} [16]; NiCoAl: 52 to 63 kcal mol^{-1} [20]).

The volume-fraction increases with increasing Ti + Al content of the alloy; however to quantify C_e, both the chemical composition of the γ' phase and the amount of Ti in primary carbides and nitrides have to be measured.

4.2. Precipitation hardening

Dislocation pairs have been observed in deformed specimens of both batches before reaching peak strength (see Figs 8 and 9), as suggested by the theory of hardening by ordered particles. The equations of Brown and Ham [9], Equations 1 to 3, explain quantitatively the ageing behaviour of our alloys, It is worthy of attention that the numerical results concerning the γ measurement by the above procedure, which are affected by the necessary approximations introduced both by con-

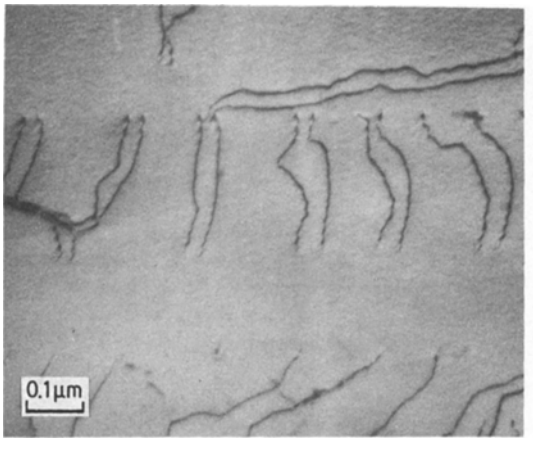

Figure 8 Dislocation pairs in Batch 760 aged for 2000 h at 575° C and deformed by about 2% in compression.

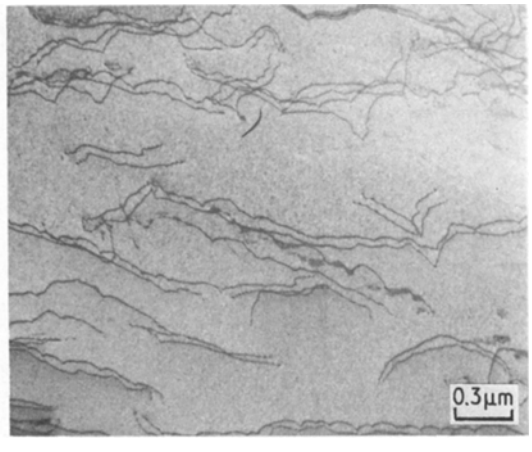

Figure 9 Dislocation pairs in Batch 761 aged for 2000 h at 575° C and deformed by about 2% in compression.

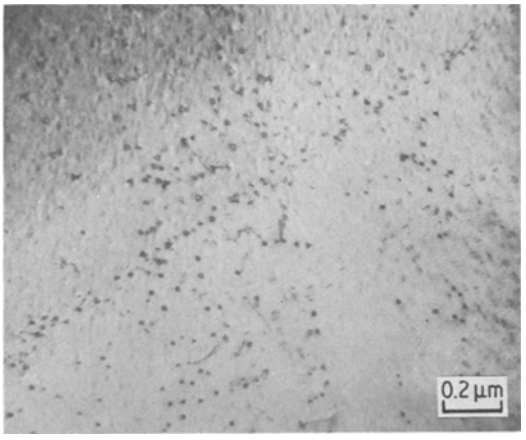

Figure 10 Orowan loops in Batch 761 aged for 2000 h at 600° C and deformed by about 2% in compression.

sidering $\Delta\tau_c = 1/2\Delta\sigma_{0.2}$ and by estimating S are able to give values of $\Delta\tau_c(r^{1/2} = 0)$, $r_s = S/\gamma$ and $\Delta\tau_c(r_s > S/\gamma)$ in quantitative agreement with the experimental data for both batches can be seen in Figs 6 and 7. Since, in $\Delta\tau_c(r^{1/2} = 0)$ and in $\Delta\tau_c(r_S > S/\gamma)$ only the $\Delta\tau_c$ estimate is involved, while in $r_s = S/\gamma$ only S appears, it can be concluded that approximations made in the analysis do not play an important role in computing γ values, so that the above procedure does not introduce large systematic errors.

It is noticed that the APB energies here obtained are greater than those measured from the age-hardening of γ/γ' alloys with lower Ti/Al ratio [5, 6] and are of the same order of magnitude as those estimated for alloys with high Ti/Al ratio [7]; this work appears to confirm that the Ti/Al ratio plays the main role in defining the APB energy of the γ' phase. In fact, in the batches investigated the APB energy also increases strongly with increasing Ti/Al ratio, as can be seen in Table III. However, in order to quantify the resulting trend the chemical composition of the γ' phase should be known; work is in progress with the aim of defining this point.

Another important conclusion of this paper is based on the agreement between the experimental data and Equations 1 to 3. This implies that appreciable contributions to hardening coming from mechanisms involving features of the particles other than order are unimportant. The significant conclusion also finds support in another detailed study devoted to this subject [5].

Single Orowan loops have been observed at the peak strength and for larger particle radii in both batches (see Fig. 10), even if the predicted stress for the Orowan process is even greater for paired dislocations (Figs 6 and 7). However, the results of the tensile tests seem to suggest that the over-ageing is mainly due to the shearing process with a $\Delta\tau_c$ given by Equation 3 and that only a few γ' particles are by-passed with the Orowan process. Additional data at longer ageing times are required in order for a conclusion to be reached concerning the hardening behaviour of Alloy 800 with large γ' particles. It is worth noting that similar age hardening behaviour has been observed for Nimonic PE-16, Ni-base alloy and its behaviour was attributed to the simultaneous occurrence of both shearing and Orowan looping [6].

6. Conclusions

The precipitation-hardening behaviour of Alloy 800 can be accounted for on the basis of the LSW theory of diffusion-controlled particle coarsening, and by the theory of shearing of ordered particles by paired dislocations, at constant particle volume-fraction at temperatures between 525 and 600° C. The Ti- and Al-contents have been found to affect the APB energy, the volume-fraction and the coarsening rate. However to quantify these effects, additional information on the chemical composition of the γ'-phase is required.

Acknowledgements

Grateful acknowledgement is made to Dr B. Dalmastri and his co-workers who performed the ageing programme and the mechanical tests.

References

1. M. JULIEN, *Nucl. Technol.* **31** (1976) 367.
2. J. ORR, Proceedings of the International Conference on Alloy 800, Petten, March 1978 (North Holland, Amsterdam, 1978) p. 25.
3. A. A. TAVASSOLI and G. COLOMBE, *Met. Trans.* **8A** (1977) 1577.
4. *Idem, ibid.* **9A** (1978) 1203.
5. V. MUNJAL and A. J. ARDELL, *Acta Met.* **23** (1975) 513.
6. V. MARTENS and E. NEMBACH, *ibid.* **23** (1975) 149.
7. D. RAYNOR and J. M. SILCOCK, *Met. Sci. J.* **4** (1970) 121.
8. H. GLEITER and E. HORNBOGEN, *Phys. Status Solidi* **12** (1965) 235.
9. L. M. BROWN and R. K. HAM, in "Strengthening Methods in Crystals" edited by A. Kelly and R. B. Nicholson (Applied Science Publishers, London, 1971) p. 12.
10. J. M. LYFSHITZ and V. U. SLYOZOV, *J. Phys.*

Chem. Sol. **19** (1961) 35.
11. C. WAGNER, *Z. Electrochem.* **65** (1961) 581.
12. C. K. L. DAVIES, P. NASH and R. N. STEVENS, *Acta Met.* **28** (1980) 179.
13. A. D. BRAILSFORD and P. W. WYNBLATT, *ibid.* **27** (1979) 489.
14. J. E. HILLIARD, *Trans. AIME* **224** (1962) 906.
15. H. GLEITER and E. HORNBOGEN, *Phys. Status Solidi* **12** (1965) 251.
16. E. H. VAN DER MOLEN, J. M. OBLAK and O. H. KRIEGE, *Met. Trans.* **2A** (1971) 1627.
17. A. J. ARDELL, *Acta Met.* **16** (1968) 511.
18. A. J. ARDELL and R. B. NICHOLSON, *ibid.* **14** (1966) 1295.
19. A. J. ARDELL, *Met. Trans.* **1A** (1970) 525.
20. C. K. L. DAVIES, P. NASH and R. N. STEVENS, *J. Mater. Sci.* **15** (1980) 1521.

Received 5 February and accepted 1 June 1981.